Applied Science and Engineering Progress, Vol. 20, No. 2, 2027, 8194

Research Article

Design of a Rice Amylose–Xanthan Gum Biopolymer Complex for Stabilisation and Encapsulation of α-Tocopherol-Loaded Pickering-Emulsion

Aininu Nafiunisa, Nita Aryanti*, Dyah Hesti Wardhani, Alifia Rizki Adina, Feni Mutiara Lasniroha Sagala and Krisan Ayu Lestari
Department of Chemical Engineering, Faculty of Engineering, Diponegoro University, Semarang 50275, Indonesia

* Corresponding author. E-mail: nita.aryanti@che.undip.ac.id DOI: 10.14416/j.asep.2026.07.001
Received: 5 February 2026; Revised: 31 March 2026; Accepted: 27 May 2026; Published online: 01 July 2025

Abstract
The encapsulation of lipophilic bioactives in emulsion systems remains a significant challenge due to limited interfacial stability and the degradation of bioactives during processing. This study elucidates the stabilization and encapsulation mechanisms of a rice amylose–xanthan gum (RAM–XG) complex as a novel pickering emulsion stabilizer for protecting α-tocopherol. FTIR analysis confirmed non-covalent complexation between RAM and XG, forming a polysaccharide network that irreversibly adsorbs at the oil–water interface. This interfacial architecture controls creaming behavior, enabling the formation of stable emulsions with an apparent droplet size of approximately 0.518 μm and stable creaming after one day of storage under optimized conditions (1:9 oil-to-water ratio, 80% ultrasonic amplitude, and 11 min processing time). During spray drying, a mechanistic trade-off between encapsulation efficiency and antioxidant preservation was observed. A higher wall material concentration (40%) enhanced the encapsulation yield (18.955%) by increasing matrix density, whereas lowering the concentration to 30% resulted in better preservation of α-tocopherol bioactivity due to reduced diffusional stress. FTIR and SEM analyses confirmed that the encapsulated α-tocopherol exhibited spherical morphology and reduced antioxidant activity. This study provides mechanistic insights into the formation of polysaccharide complex-stabilized Pickering emulsions through the regulation of particle interfacial behavior, thereby enhancing the preservation of bioactive compounds. It also offers a logical framework and fundamental understanding for designing delivery systems for hydrophobic nutraceuticals.

Keywords: Antioxidant, Complexation, Droplet stability, Encapsulation, Ultrasonic emulsification

1 Introduction

Responding to the demand for health-promoting foods, food manufacturers compete to develop better food products with added functional value. α-Tocopherol is among the most studied bioactive compounds for food fortification and nutrification due to its numerous health benefits, including anti-inflammatory and antioxidant effects [1]. Despite the benefits of α-tocopherol for human health, its fortification poses significant challenges because of the poor solubility in aqueous matrices and its susceptibility to oxidative degradation during processing and storage under light, heat, and oxygen [2], [3]. To overcome these hurdles, incorporating α-tocopherol into emulsion-based systems has been reported to be an effective solution in previous studies [4–6]. Based on this system, several crucial factors must be addressed to effectively protect the loaded α-tocopherol, including emulsion stability and encapsulation efficiency [7]. The emulsion should be able to sustain against instability and droplet breakup. At the same time, the emulsifier should also act as an encapsulant, protecting α-tocopherol from degradation and preventing interactions with oxygen. Given the desired system and prior studies, pickering emulsion is the best [8]. Pickering emulsion is the emulsion system stabilized by solid particles, including natural or synthetic particles [9]. The particles used in stabilizing pickering emulsion were characterized with a contact angle of ~90°, which is able to stay on the interface layer of oil and water [10]. Pickering emulsion is known to have enhanced stability, better cost-effectiveness, versatile functionality and foremost can be easily made from natural materials [11].

Pickering emulsion stabilized by natural based stabilizer is way safer than the synthetic surfactants [8].

Applied Science and Engineering Progress, Vol. 20, No. 2, 2027, 8194

The previous study has studied the use of several natural materials as the emulsion stabilizer applied for encapsulation of lipophilic bioactive ingredients, such as caseinate/alginate [12], chayote tuber starch [9], *Pueraria lobata* nano-starch [13], and modified chitosan [14], [15]. Nowadays, particles of starch have been studied as emulsion stabilizers with better accessibility, health benefits, less environmental impact, and higher sustainability than synthetic particles [16]–[18].

Starch-based emulsions are stabilized using steric hindrance, which involves the stabilization of the emulsion droplets using a steric stabilizer, thus preventing the droplets from coalescing [19]. In this case, the slow digestibility and resistance of amylose to gastrointestinal degradation allow for the controlled release and intestinal bioavailability of lipophilic compounds, including α-tocopherol [18]. Thus, high-amylose starch has been studied for its application as a dual-purpose material, stabilizer and emulsifier, although high-amylose starch (>40% amylose) is not readily available and is expensive [20]. In order to obtain amylose-rich moieties, the gelatinized nonwaxy rice starch can be isolated using a simple heat-induced process. In this case, rice starch was used due to its intermediate amylose content (12-28%) and small granule size [21]. The isolated needle-like crystalline structures are related to the hydrophobic amylose domains, which are advantageous for the stabilization of Pickering emulsions [22]. In this study, the amylose content extracted from rice starch was used as the emulsion stabilizer, named as rice amylose moieties (RAM). However, the application of a single stabilization mechanism may not be sufficient for the simultaneous stabilization of the emulsion and the bioactive compounds.

Therefore, the application of a dual mechanism stabilization approach is essential for achieving enhanced physical stability and bioactive protection by α-tocopherol. Previous studies have reported the application of modified starch for enhanced emulsion stability [10], [17], [20], [23]; however, the study on the bioactive protection in solid powder form has not been taken into consideration comprehensively. On the other hand, most other studies on the bioactive protection were applying the complex of polysaccharides and protein in Pickering emulsion, such as whey protein/pectin [24], soy protein/sodium alginate, soy protein/xanthan gum [25], casein/hyaluronic acid [26], BSA/xanthan gum and others [27]. On the contrary, the application of polysaccharide-polysaccharide or polysaccharide-hydrocolloid complexes has gained significant attention due to the enhanced physical stability of the emulsions [8], [28].

Xanthan gum (XG), an anionic polysaccharide, has been used as an effective non-adsorbing hydrocolloid for the stabilization of emulsions by increasing the viscosity of the continuous phase of the emulsion and slowing the rate of creaming of the emulsion droplets [29], [30]. In the present investigation, a polysaccharide complex made from RAM and XG has been made for the development of a dual function stabilizer for the Pickering emulsion, which includes the application of the Pickering stabilization approach along with the application of the non-adsorbing hydrocolloid approach for the stabilization of emulsions. RAM has been used for the entrapment of α-tocopherol within the helical structure of the polysaccharide, thus restricting the extent of oxidative degradation of the bioactive [31]. XG has been applied for the control of the dynamics of the emulsion droplets by increasing the viscosity of the continuous phase of the emulsion [32].

In addition, the ultrasonic emulsification process gives higher stability to the resulting emulsion. The mechanochemical effects induced by ultrasonication contribute to the encapsulation properties of the stabilizer materials [33]. Consequently, this procedure can enhance ingredient management, preventing adverse reactions and undesired interactions among the active compounds. The investigation regarding the stabilization of α-tocopherol-loaded emulsion using the complex of RAM and XG, along with ultrasonic-assisted emulsification, has not been previously conducted. Moreover, the influence of the emulsification condition on the stability of the mentioned emulsion system has not been studied elsewhere before. Hence, an in-depth study of this research is warranted. The present study investigates the stability of the emulsion stabilized by the novel complex of RAM/XG under various ultrasonic emulsification conditions, followed by an evaluation of the interfacial activity mechanism of the RAM/XG complexes to stabilize the emulsion and protect α-tocopherol synergistically. The work also studies the ability of the mentioned emulsion system to stabilize the loaded α-tocopherol under both emulsion and dry encapsulation. The study results are believed to provide a theoretical framework for applying Pickering emulsion as an efficient system to fortify bioactive compounds in food products.

2 Materials and Methods

2.1 *Materials*

The study used rice starch (PT. Dwi Asoka Multisains, Indonesia) and food-grade xanthan gum (Neimenggu Fufeng Biotechnologies Co. Ltd., China). The α-tocopherol (99.9% purity, Merck, Singapore) was used as the bioactive compound. Sunflower oil (Golden Bridge, Malaysia) as the continuous phase. Other chemicals of HCl, NaOH, maltodextrin, etc., were procured from a local chemical distributor in technical standard. Distilled water was used as the solvent throughout the experiments.

2.2 *Emulsification*

2.2.1 Preparation of stabilizer

The amylose-rich moieties were extracted from rice starch as per a previously described method with minor modifications [34]. To summarize, rice starch solution (5% w/v) was prepared using distilled water, soaked in water for 30 minutes at room temperature to hydrate, gelatinized at 90 °C with stirring at 250 rpm for 20 minutes, cooled to room temperature, followed by centrifugation at 3900 rpm for 30 minutes. The supernatant solution rich in extracted amylose moieties was used immediately for the further complexation process. For complex formation, the solution of RAM and a 1% (w/v) solution of XG at a ratio of 1:1 (v/v) were allowed to stand at room temperature for 48 hours in the absence of stirring [28]. The solution of the complex of RAM and XG was then used directly as the continuous phase for emulsification.

2.2.2 Formation of coarse emulsion

A coarse emulsion was formed by homogenization, at oil-water ratios of 1:9 using a rotor-stator homogenizer (DLAB handheld homogenizer, D-160, China) at 11,000 rpm for 5 minutes. The resulting emulsion was used for further analysis.

2.2.3 Formation of fine emulsion by ultrasonication

Coarse emulsion was converted into fine emulsion by the induction of ultrasonic waves using a probe ultrasonic processor (900-92, Biosafer, China) for specific times (7, 9, and 11 minutes). This range of time was selected as the emulsion started to form at this time range, while keeping no over-processed droplet breakup [35]. While the amplitudes vary at 40%, 60%, and 80%, that will give sonication power of 360, 540, and 720 W, consequently. This power range is enough to break the coarse droplet into a fine emulsion [36]. Processing time and sonication power, shown by amplitude, are chosen as these variables are known to directly affect the breaking up of droplets and the stability of an emulsion [37]. To prevent overheating, emulsification was conducted in an ice-water bath using pulse mode (2 s on/4 s off).

2.3 *Preparation of α-tocopherol-loaded emulsion*

α-tocopherol (5, 10, and 15% w/w) was dissolved in the oil phase using a stirrer at 2000 rpm for 5 minutes and then used as the dispersed phase to perform the emulsification process as mentioned in Section 2.2.3. The prepared emulsion samples were kept for stability evaluation. For the encapsulation process, another batch of the emulsion sample was added with maltodextrin (30, 35 and 40% w/w) and then spray-dried at an inlet and outlet temperature of 160/80°C with a feed rate of 5 mL/min. The samples were kept in dark airtight containers at 4°C.

2.4 *Analysis of RAM/XG complexes*

The RAM/XG complexes were characterized in solution with respect to particle size and functional groups. The average particle size of RAM/XG complexes was determined using a particle size analyzer (Labtron, LLPA-C10, UK), and dynamic light scattering was performed at a wavelength of 633 nm without any further sample dilution. FT-IR spectra of RAM/XG complexes were recorded using a PerkinElmer UATR Spectrum Two (USA) within a wavenumber range of 400-4000 cm^{-1}.

2.5 *Emulsion stability analysis*

Emulsion stability was evaluated by studying time-dependent creaming, droplet size changes, turbidity, and centrifugal stability. Each analysis was conducted for each sample along the storage time for 14 days, to show the changed on the emulsion during the storage. Droplet size and morphology were evaluated by optical microscopy analysis combined with image processing software. This study is widely used for comparative assessment of emulsion systems [38], [39]. Particularly, in observing the effect of processing

Applied Science and Engineering Progress, Vol. 20, No. 2, 2027, 8194

conditions on the droplet disruption and distribution, which is the focus of the present study.

Prior to analysis, the emulsion upper layer was diluted tenfold with distilled water, and 20 µL of the sample was deposited on a microscope slide. Optical microscopic images of the sample were recorded, and the droplet size was evaluated by using a CCD camera. At least 300 droplets were evaluated using ImageRaster software, and the average droplet diameter (d_{avg}) was evaluated using Eq. (1) with the help of OriginPro software. Where d_i is the diameter of each droplet, and N is the total number of droplets [39]. Due to the resolution limitations of optical microscopy for submicron measurements, the submicron results are primarily used for comparative analysis rather than exact size determination.

$$d_{avg} = \sum_{i=1}^{n} d_i / N \quad (1)$$

Creaming stability was quantitatively assessed using the creaming index (CI) measured in accordance with the method described in reference [39]. The height of the formed cream layer at the top and the remaining water layer at the bottom was measured. Then, the CI was calculated as the percentage of the remaining water layer to the total height of the total emulsion [39]. For the determination of the turbidity stability, the absorbance of the lower emulsion layer at 600 nm was measured with a UV-Vis spectrophotometer after the buffer solution was used as a blank solution. The turbidity (T) was calculated from the absorbance value (A_0) as described in Eq. (2), with the scattering path length (CL) of 1 cm.

$$\mathrm{T} = (2.303 \times A_0)/\mathrm{CL} \quad (2)$$

Meanwhile, the centrifugation stability test was conducted by taking 0.2 ml of the emulsion, diluted 50 times, and analyzed using a UV-Vis spectrophotometer at 500 nm to get the initial absorbance (A_0). The diluted emulsion was then centrifuged (20 min, 3000 rpm). Then, the absorbance of the resulting bottom layer (A_i) was also calculated on the UV-Vis spectrophotometer at a wavelength of 500 nm. The centrifugation value (Ke) is calculated referring to Eq. (3) [40].

$$Ke = (A_i - A_0/A_i) \times 100\% \quad (3)$$

The viscosity of the prepared emulsion was calculated right after the emulsion preparation (d_0) and after 14 days of storage in room conditions (d_i). The Ostwald viscometer was employed to determine the viscosity of the emulsion, using water as the standard fluid [41].

2.6 *Characterization of the encapsulated α-tocopherol*

α-Tocopherol-loaded powders were studied for their micromorphology, particle size, and antioxidant activity. Micromorphology was studied using low vacuum scanning electron microscopy (SEM) at 5000x magnification after sputter coating the powders with 200 Å gold using low vacuum SEM (JSM-6510LA, JEOL Ltd., Japan). Particle size was studied using a particle size analyzer as described in Section 2.4. Antioxidant activity was studied using the DPPH free radical scavenging method [3,42]. For this purpose, 100 µg/mL DPPH solution was used as the control. Then, the encapsulated powder was re-dispersed in ethanol at a concentration of 25 - 100 µg/mL, expressed based on total powder mass. The sample solutions were stirred before analysis. To 4 mL of each sample, 1 mL DPPH solution was added and incubated for 30 minutes in the dark. Absorbance was then measured at 515 nm. The percentage inhibition was calculated using Eq. (4), and IC50 values were calculated by linear interpolation for 50% inhibition values [43].

$$\%IC50 = \frac{Abs_{DPPH} - Abs_{sample}}{Abs_{DPPH}} \times 100\% \quad (4)$$

3 Result and Discussion

3.1 *Characteristic of stabilizer*

Figure 1 shows the structural changes and intermolecular interactions between RAM and XG, as characterized by FTIR spectra. The spectra of pure RAM and XG showed characteristic peaks corresponding to their respective functional groups. Specifically, the FTIR spectrum of pure RAM showed typical peaks associated with the amylose backbone, with peaks observed in the 1300-900 cm^{-1} region [44]. The peaks for the C–C stretching and C–O bending vibrations for amylose were observed at 1145 and 997 cm^{-1}, respectively [45]. The spectrum of C–H stretch and broad –OH stretching of RAM at 2937 and 3285 cm^{-1}, respectively, represents the D-glucose chain [18]. The FTIR spectrum for the RAM/XG complex showed characteristic peaks for the amylose backbone, with peaks for the C–C and C–O vibrations observed at 1146 and 995 cm^{-1}, respectively. XG exhibited characteristic bands at 1025, 1602, 2887, and

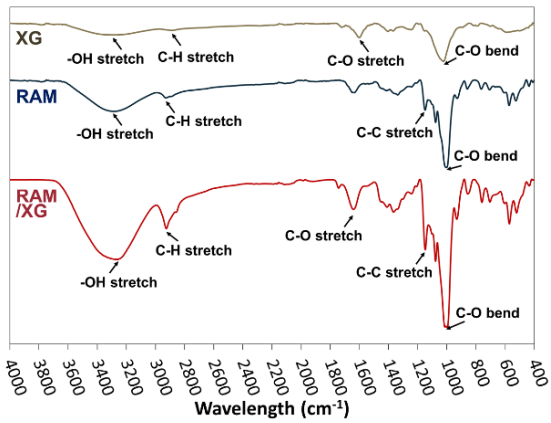

Figure 1: FTIR spectrum of RAM/XG complex.

3269 cm^{-1}, assigned to C–O bending of acetate groups, C–O stretching of carboxyl groups, C–H stretching, and –OH stretching, respectively [40]. The presence of these peaks in the RAM/XG spectrum confirms that the complex retains the structural features of both components.

Figure 1 also shows several peak shifting and intensity changes compared to the native materials, suggesting that RAM interacts with XG via hydrogen bonds, steric effects, and molecular entanglements. Both XG and RAM have abundant ─OH groups that can form hydrogen bonds with each other. Interaction between ─OH groups on the amylose glucose units with XG is confirmed by the ─OH peak shifting to the lower wavenumber at 3263 cm^{-1}; accompanied by peak broadening and increased intensity compared to native RAM and XG, indicating stronger hydrogen bonding in the complex [27]. Additionally, the C–H stretch peak at 2926 cm^{-1} also shows red shifting and higher intensity than the individual RAM and XG. A change in this region indicates conformational changes in the polymers due to their interaction [25]. Furthermore, the carboxyl groups of the XG may also participate in the hydrogen bonding with the –OH groups of RAMs. This phenomenon is indicated by the shift and increase of peak intensity in the carboxyl groups (asymmetric stretching ─COO) at 1642 cm^{-1}.

The complexation of the RAM and XG can also be verified by comparing the band ratio of the native XG with that of the RAM/XG. The change in the band ratio of the native XG after complexation shows that there are changes in its molecular structure due to interaction, conformational state, or other factors. Table 1 summarizes the band ratios of several correlated absorption bands. The ratio of ─OH/C─H bands of the complex shows a lower value than the native XG; this can happen due to the increase of C─H in the glucose backbone and side chains, leading to structural changes in the complex. In addition, the ratio of the C─O stretch/C─H stretch bands also shows a decrease in the RAM/XG spectrum compared to the native XG. The C─O stretch band represents the stretching vibration of the glycosidic bonds in the native XG compared to the RAM/XG complex.

Meanwhile, the C-H stretch vibration represents the glucose chain, which increases after complexation with RAM. A decrease in band ratio between these bands reflects a molecular interaction in the backbone of the XG structure. The previous study also discusses the confirmation of complexation between XG and native potato starch based on the band ratio change within a specific wavelength, where the change of band ratio was found even with the simple mixture complexation process [30]. The schematic of the possible complexation mechanism between RAM/XG is depicted in Figure 2.

3.2 *Effect of ultrasonication power and periods on the characteristics of the RAM/XG emulsion*

The advanced emulsification utilizing ultrasonic waves enables the production of a smaller droplet size and a more stable emulsion. The influence of ultrasonication on the emulsion stability is presented in Figure 3.

Table 1: FTIR band ratio of native XG and RAM/XG complex.

Ratio	Functional Groups	XG			RAM/ XG		
		Wavenumber (cm^{-1})	%T	Band Ratio	Wavenumber (cm^{-1})	%T	Band Ratio
R1	-OH stretch	3269	94.27	0.962	3263	67.64	0.850
	C-H stretch	2887	98.02		2926	79.56	
R2	C-O stretch	1025	84.05	0.875	1078	66.94	0.841
	C-H stretch	2887	96.02		2926	79.56	
R3	~1250 (C-O)	1246	96.28	1.005	1243	92.98	1.082
	~1375 (C-H)	1369	95.81		1367	85.91	

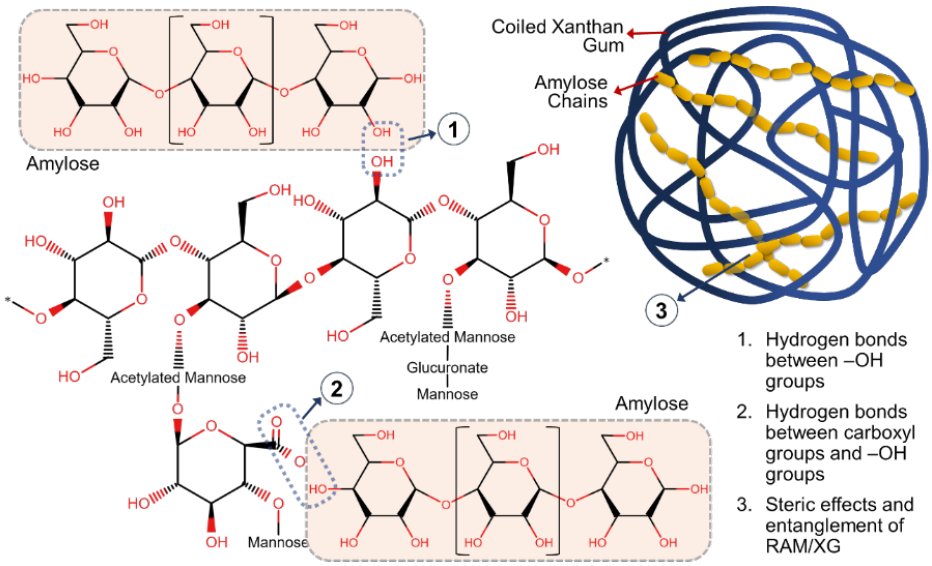

Figure 2: Schematic complexation mechanism of RAM/XG.

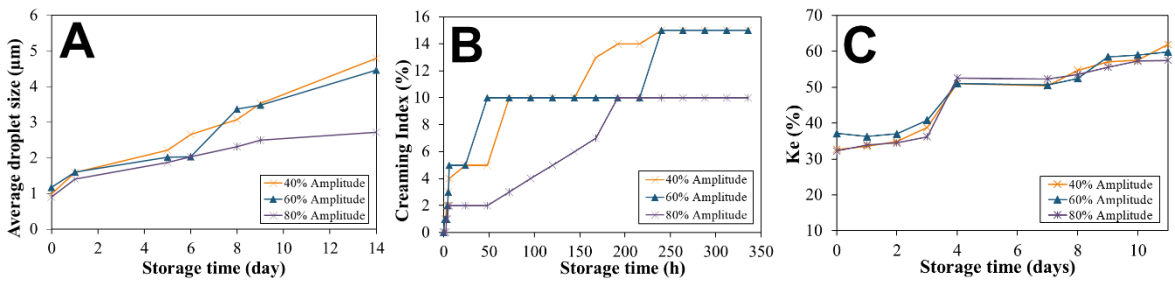

Figure 3: Effect of ultrasonic amplitude at a fixed ultrasonication time of 7 min, oil-to-water ratio of 1:9 and without α-tocopherol on (a) average diameter of the droplet, (b) creaming index, and (c) centrifugation stability (*Ke*) of the emulsions.

The change in ultrasonic power was most prominently affecting the droplet size and CI. Notably, the emulsion prepared at 80% ultrasonic amplitude generates smaller droplet sizes compared to the 40% and 60%. Increased processing power results in smaller particle sizes due to reduced energy density [46]. Ultrasonic cavitation, arising from alternating low-pressure and high-pressure bubbles, facilitates the breakdown of the droplet into smaller sizes. In line with the prior study, our findings affirm an inverse relationship between amplitude and droplet size, with greater amplitude yielding smaller droplet sizes [47]. This correlation extends to creaming stability, where a higher amplitude corresponds to a smaller creaming index (Figure 3B). This improvement is attributed to enhanced droplet uniformity and reduced aggregation induced by high-power ultrasonication. This generates smaller and more homogeneous droplets at the optimized condition. Even though the submicron droplet size was estimated from an optical microscopy analysis, this method remains used in several studies to evaluate emulsion droplet size, especially for comparative purposes [38], [48–50]. The previous study has also compared the submicron droplet size obtained from optical microscopy and direct light scattering (DLS), which showed a linear result between the two methods [38]. As a result, the reported value should be seen as an approximate estimate that is meant to show how processing conditions affect droplet size reduction rather than as an exact measurement.

According to Stokes' law, smaller droplets experience lower buoyant forces and rise more slowly, thereby suppressing oil droplet migration into the cream layer [51]. Additionally, smaller droplets provide a larger interfacial surface area for the adsorption of RAM/XG. Consistent with the CI profile, the change in the

ultrasonic amplitude affects the turbidity of the fresh emulsion (day 0). This effect is related to the production of smaller droplets in micron size by increasing ultrasonic power, which scatter light more effectively, leading to the increased of turbidity in emulsions [46]. As well as an increased total droplet number resulting from the breakup of larger droplets during ultrasonication.

Interestingly, centrifugal stability remained unaffected by increasing the ultrasonic power (Figure 3C), despite noticeable changes in other stability parameters. Centrifugal stability reflects the resistance of the emulsion against phase separation under the impact of centrifugal force [40]. No change in the Ke value indicated the ability of the RAM/XG complex to prevent droplet coalescence and sedimentation. The increase of ultrasonic power primarily affects the droplet size by breaking down larger droplets into smaller ones through the breakup of cavitation bubbles [5]. However, it does not necessarily improve the interfacial stabilization provided by the stabilizers. When the stabilizer has optimal coverage, the interface of the droplets, even at lower ultrasonic power, increasing the power will not further enhance the emulsion stability [46]. Moreover, centrifugal stability was calculated based on the turbidity of the cream layer after centrifugation [40]. Thus, even though a cream layer formed, the stabilizer effectively prevented droplet coalescence, maintaining turbidity and yielding comparable centrifugal stability values. The emulsion viscosity decreased with increasing ultrasonic amplitude (Figure S1). Viscosity is closely related to droplet population and structure, with higher values generally associated with a greater number of dispersed droplets. Viscosity reduction over time is attributed to droplet breakup into smaller sizes induced by higher ultrasonic amplitude and prolonged ultrasonication, as well as gradual dilution effects during storage.

A further investigation was conducted to study the effect of ultrasonication periods on the emulsion characteristics and stability (Figure 4 and S2). Longer ultrasonication periods significantly improved the creaming stability. The emulsions prepared at 11 minutes of ultrasonication showed the most stable creaming after only one day of storage. Prolonged ultrasonication improves the interaction and distribution of the complex stabilizer, enhancing the strength of the interfacial layer that covers oil droplets [52]. In addition, XG forms a gel-like network in the aqueous phase [32]. Longer ultrasonication may improve its dispersion and interaction with starch amylose, strengthening the networks that trap the oil droplets and prevent creaming. The effect of an extended period of ultrasonication in improving the stability of emulsions has been proven in other research studies [52].

However, prolonging the ultrasonication time did not significantly influence droplet size and centrifugal stability. This was due to the mechanical dismantling that occurs during the emulsification process, resulting in less interfacial stabilization [40]. Ultrasonication time primarily affects the initial droplet breakup [33], and when the droplets become sufficiently small, sonication has no significant effect on reducing the size of droplets. Moreover, if the stabilizers are already effectively covering the oil-water interface, additional ultrasonication time will not further reduce droplet size. Time-dependent stability analysis shows that the emulsion produced at 11 min ultrasonication shows eminent stabilization, as shown by an unchanged droplet size after 5 days of storage.

3.3 *Effect of α-tocopherol concentration on the characteristics and stability of the emulsion*

The addition of α-tocopherol to the oil phase of the emulsion increases the droplet size and reduces the turbidity (Figure 5**)**. This phenomenon is related to the viscosity difference between α-Tocopherol and the carrier oils [29]. Dissolution of hydrophobic α-Tocopherol increases the viscosity of the loaded oil phase, preventing droplet breakups during emulsification. Resulting in larger droplet sizes and less dispersed droplets, induced lees light scatter compared to smaller and packed droplets, resulting in lower turbidity. A similar result was also found in the previous study, where higher α-tocopherol addition increases the viscosity and droplet size of the emulsion, and the addition of tocopherol should be limited under 5% of volume to prevent alteration of the emulsion characteristic [41].

α-tocopherol addition also promotes emulsion instability. Figure 5B shows that the 5%-loaded emulsion shows stable creaming after 5 days of storage at CI of 20%, which 80% longer and 2 times higher than the unloaded emulsion. Moreover, the loaded emulsion also shows a further increase in droplet size along the storage time and reaches the stable point after 9 days of storage, 2.25 times longer than the unloaded emulsion, which reaches the stable droplet size after 5 days of storage. The mechanism behind this phenomenon may be related to the α-Tocopherol competition with the stabilizer at the oil-water interface and weakened the interfacial film.

Applied Science and Engineering Progress, Vol. 20, No. 2, 2027, 8194

RAM/XG complex forms a network that stabilizes oil droplets by increasing viscosity and forming a steric barrier. However, amphiphilic α-Tocopherol may insert itself into the interfacial layer, potentially disrupting the structured stabilization provided by the biopolymer complex [27]. This could reduce steric repulsion between droplets, leading to droplet coalescence. α-Tocopherol interaction may also happen on both sides of the complex. Amylose has a hydrophobic cavity that can interact with nonpolar molecules like α-Tocopherol [44]. While α-Tocopherol may alter the molecular conformation of the XG by affecting its hydration shell or ionic interaction, it provides less electrostatic repulsion and hydration properties. This alteration then led to weaker droplet stabilization and lower interfacial surface for adsorption. This interaction also changes the rheology of the continuous phase shows by the viscosity change upon tocopherol addition (Figure S3).

Furthermore, despite the increase in droplet size, faster creaming, and lower turbidity, loading α-Tocopherol on the emulsion did not completely destabilize it. This was shown by the insignificant change in the centrifugal stability with the increase of α-tocopherol addition (Figure 5C). This indicates that even though α-Tocopherol causes changes at the interface, it does not seem to break down the emulsion structure completely. Moreover, the bulk phase still contains a sufficient number of networks of the RAM/XG complex, which still provides enough structural stability and remains robust enough to maintain the structural integrity, allowing the system to remain stable under centrifugal stress.

3.4 *Characteristics of encapsulated α-tocopherol*

Figure 6A presents the morphology of the encapsulated α-tocopherol. Spray drying typically produces spherical particles due to rapid solvent evaporation and surface tension–driven droplet formation [53]. In this study, SEM analysis showed that particle morphology was strongly influenced by the wall material concentration. At 30 and 35% maltodextrin, the encapsulated powders exhibited homogeneous and relatively uniform spherical structures, indicating effective α-tocopherol encapsulation and stable droplet formation during spray drying. This morphology suggests that these concentrations provide an optimal balance between feed viscosity and drying kinetics, promoting the formation of well-defined particles [53].

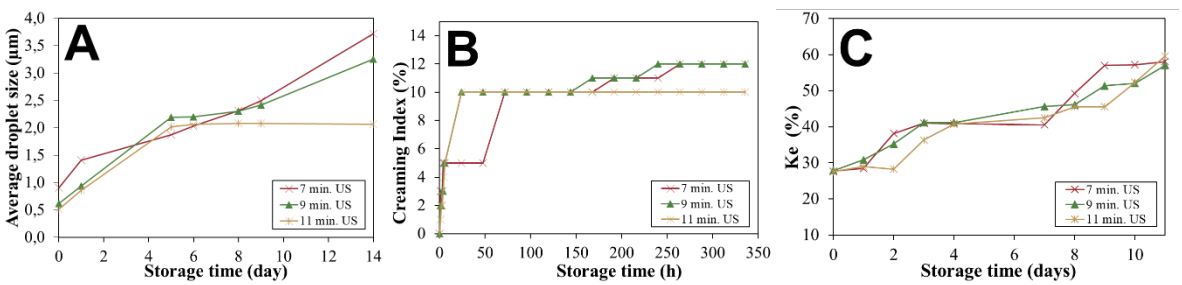

Figure 4: Effect of ultrasonication time at a fixed ultrasonic amplitude of 80% min, oil-to-water ratio of 1:9 and without α-tocopherol on (a) average diameter of the droplet, (b) creaming index, and (c) centrifugation stability (*Ke*) of the emulsion

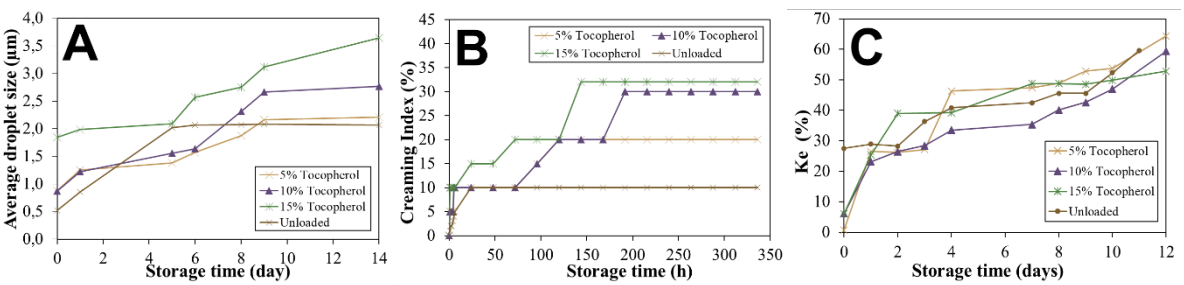

Figure 5: Effect of α-tocopherol concentration at a fixed ultrasonic amplitude of 80%, ultrasonication time of 11 min and oil-to-water ratio of 1:9 on (a) average droplet diameter, (b) creaming index, (c) centrifugation stability (*Ke*) of the emulsions.

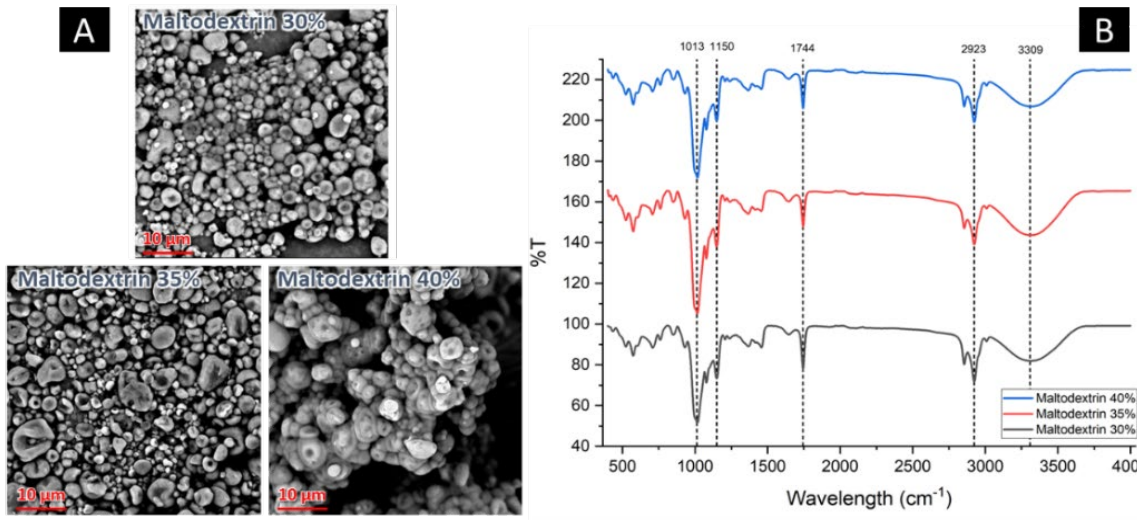

Figure 6: SEM analysis (A), FTIR analysis (B) of the loaded emulsion powder.

In contrast, increasing maltodextrin concentration to 40% resulted in irregular particle shapes and non-uniform sizes, which are attributed to elevated feed viscosity that hinders droplet atomization and promotes incomplete drying or particle agglomeration. These observations are consistent with previous reports showing that excessive wall material concentration adversely affects particle morphology by altering viscosity and drying behavior [54]. The result was also supported by the particle size analysis, shows on Figure 7(A)**.** Where dry powder produced at 30 and 35% maltodextrin has a narrower size distribution and lower PDI compared to the encapsulate powder with 40% addition of maltodextrin. The average droplet sizes of 30%; 35%, and 40% maltodextrin are 3.927, 3.749, and 3.782 µm, respectively.

The FTIR spectra of the particle powders are shown in Figure 6B. The previous study reveals that the FTIR spectrum of the pure α-tocopherol displayed several specific characteristics. Presented by, C-O bond, C=C bond, C=O stretching vibration, C-H alkane groups, terminal hydroxyl groups and C–O stretching groups [55]. Comparing the FTIR spectra of the dry α-tocopherol-loaded emulsion with the pure α-tocopherol revealed four matching peaks. Firstly, the loaded emulsion shows the peaks of –OH bond at 3309 cm^{-1}, and vibration of C–H at 2923 $cm^{-1,}$ indicating the methyl group of tocopherols. Additionally, the emulsified tocopherol also shows C=O stretching vibration peak at 944–1065 cm^{-1} and C–O stretching at 1150 cm^{-1}. Based on the FTIR results, it can be concluded that α-tocopherol is effectively preserved within the product, as evidenced by the matching peaks and characteristic vibrations observed on the spectrum.

The yield analysis results indicate that the choice of coating materials significantly affects the encapsulation yield (EY), as shown in Figure 7(B). EY represents the percentage of encapsulated product relative to the total materials used, with higher values indicating a more efficient process. Several factors influence encapsulation efficiency, including wall and core materials, emulsion properties, and the spray drying process. Emulsion stability plays a key role, as better stability improves encapsulation efficiency [56]. Nevertheless, the rise in emulsion viscosity decreases the duration required for the formation of a semipermeable membrane or outer shell around the atomized droplets during the initial phase of the drying process. This could affect the encapsulation efficiency as XG complexes improve emulsion stability by increasing the viscosity of the continuous phase.

In this study, a coating emulsion with 40% maltodextrin provided the best concentration and ratio for encapsulation. While other variables only achieved relatively low EY of 12.576% and 18.955% for the encapsulated product with 35% and 40% maltodextrin, respectively. For that reason, maintaining an appropriate maltodextrin-to-core material ratio is crucial for optimizing yield. Low EY can be related to several factors occurred during the drying process. During the spray drying process, exposure to heat and atomization may contribute to degraded and volatilized the sensitive component from the feed solution [57]. Moreover,

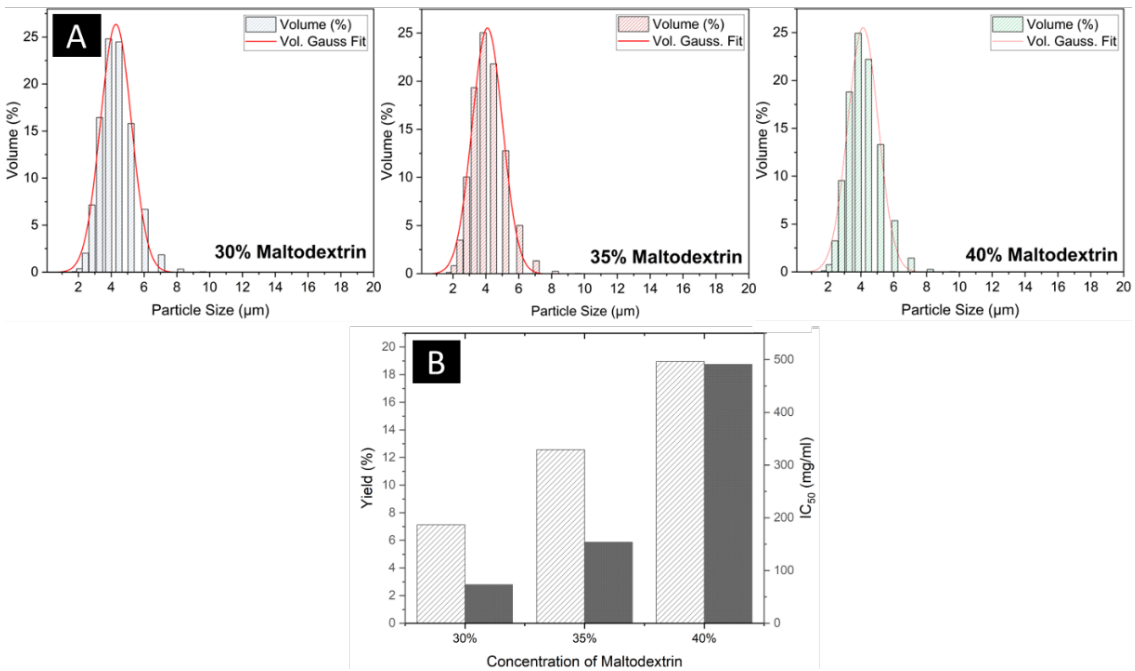

Figure 7. Average particle size (A), yield, and antioxidant activity (B) of the loaded emulsion powder.

material loss can also happen when the produced powder sticks to the walls of the drying chamber and cyclone, which commonly happens during a laboratory-scale spray drying process [58]. Despite the relatively low yield, similar ranges have been reported in spray-dried emulsion systems by Ribeiro *et. al.*, who found that encapsulating α-tocopherol resulted in a 19.20% EY, whereas formulations without α-tocopherol achieved 35.03% [4].

The antioxidant activity (AA) of the encapsulated α-tocopherol (Figure 7(B)), measured using the DPPH method, revealed that pure α-tocopherol and emulsified α-tocopherol exhibited very strong AA, as indicated by their low IC50 values [59]. However, when encapsulated with maltodextrin, the AA decreased progressively with higher maltodextrin concentrations: 30% maltodextrin yielded strong AA, 35% resulted in average AA, and 40% led to weak AA. This decline in AA can be attributed to the dilution effect of maltodextrin, which increases total solids without contributing to antioxidant capacity. As maltodextrin concentration rises, the relative proportion of α-tocopherol decreases, reducing its effective concentration and, consequently, its AA. Additionally, the encapsulation process may limit the accessibility of α-tocopherol to DPPH radicals, further diminishing the measured AA [14]. These mechanisms explain the observed reduction in AA with higher maltodextrin concentrations.

4 Conclusion

This study demonstrates that the RAM–XG complex functions as an effective Pickering emulsion stabilizer through a non-covalent polysaccharide network that irreversibly adsorbs at the oil–water interface. FTIR analysis confirmed that hydrogen bonding and molecular entanglement govern complex formation, which in turn regulates interfacial coverage, droplet breakup, and creaming behavior. The resulting interfacial architecture enabled the formation of highly stable emulsions under optimized processing conditions. This optimized condition consisted of an oil/water ratio of 1:9, an ultrasonic amplitude of 80% and ultrasonication time of 11 min. Which, resulted on a stable emulsion characterized by small droplet size (~0.518 µm, estimated from optical microscopy), low creaming index (10% after 24 h) and stable under centrifugation force. When applied to α-tocopherol encapsulation, the spray-drying process revealed a mechanistic trade-off between encapsulation efficiency and bioactive preservation. Higher maltodextrin concentration (40%) enhanced encapsulation yield by increasing matrix density,

whereas lower concentrations better preserved antioxidant activity by reducing diffusional limitations and processing-induced degradation, as validated by FTIR and SEM analysis. These findings highlight that emulsion stability and bioactive retention are governed not only by formulation composition but also by interfacial and matrix-level mechanisms Overall, this work provides mechanistic insight into how starch–polysaccharide complex particles control emulsion stability and encapsulation performance. This information can be used to design better ways to deliver lipophilic nutraceuticals. As a suggestion, future research must focus on storage stability, re-dispersibility, and process reproducibility to enhance its validation for practical applications.

Acknowledgment

This work was supported and funded by Indonesian Ministry of Education, Culture, Research and Technology through scheme of doctoral research (PDD) (Grant No: 449A-09/UN7.D2/PP/VI/2023).

Author Contributions

A.N.: conceptualization, writing – reviewing and editing, research design; N.A.: conceptualization, validation, funding acquisition; D.H.W.: methodology, supervision, A.R.A.: data curation, project administration; F.M.L.S.: formal analysis, investigation, writing–original draft preparation; K.A.L.: formal analysis, investigation, writing–original draft preparation. All authors have read and agreed to the published version of the manuscript.

Conflicts of Interest

The authors declare no conflict of interest.

Declaration of generative AI and AI-assisted technologies in the writing process

The authors utilized the assistance of AI-tools (ChatGPT and Grammarly) to enhance the language and readability of the manuscript.

References

[1] P. Borel, O. Dangles, and R. E. Kopec, "Fat-soluble vitamin and phytochemical metabolites: Production, gastrointestinal absorption, and health effects," *Progress in Lipid Research*, vol. 90, Jun. 2023, Art. no. 101220, doi: 10.1016/j.plipres.2023.101220.

[2] C. M. Sabliov et al., "Effects of temperature and UV light on degradation of α-tocopherol in free and dissolved form," *Journal of the American Oil Chemists' Society*, vol. 86, no. 9, pp. 895–902, Sep. 2009, doi: 10.1007/s11746-009-1411-6.

[3] J. R. Hyatt, S. Zhang, and C. C. Akoh, "Comparison of antioxidant activities of selected phenolic compounds in O/W emulsions and bulk oil," *Food Chemistry*, vol. 349, 2021, art. no. 129037, doi: 10.1016/j.foodchem.2021.129037.

[4] A. M. Ribeiro, B. N. Estevinho, and F. Rocha, "Improvement of vitamin E microencapsulation and release using different biopolymers as encapsulating agents," *Food and Bioproducts Processing*, vol. 130, 2021, pp. 23–33, doi: 10.1016/j.fbp.2021.08.008.

[5] R. Rashid, F. A. Masoodi, S. M. Wani, S. Manzoor, and A. Gull, "Ultrasound assisted extraction of bioactive compounds from pomegranate peel, their nanoencapsulation and application for improvement in shelf life extension of edible oils," *Food Chemistry*, vol. 385, Mar. 2022, Art. no. 132608, doi: 10.1016/j.foodchem.2022.132608.

[6] C. Cheng, C. Yuan, B. Cui, J. Li, and G. Liu, "β-Cyclodextrin based Pickering emulsions for α-tocopherol delivery: Antioxidation stability and bioaccessibility," *Food Chemistry*, vol. 438, 2024, Art. no. 138000, doi: 10.1016/j.foodchem.2023.138000.

[7] I. Sarvan, A. Jürgensen, M. Greiner, and O. Lindtner, "How long can you store vitamins? Stability of tocopherols and tocotrienol during different storage conditions in broccoli and blueberries," *Food Chemistry: X*, vol. 22, May 2024, Art. no. 101444, doi: 10.1016/j.fochx.2024.101444.

[8] X. Ren, C. Zhou, A. Qayum, J. Tang, and Q. Liang, "Pickering emulsion: A multi-scale stabilization mechanism based on modified lotus root starch/xanthan gum nanoparticles," *International Journal of Biological Macromolecules*, vol. 233, Jan. 2023, Art. no. 123459, doi: 10.1016/j.ijbiomac.2023.123459.

[9] X. Wang et al., "Enhanced stability and antioxidant activity of Pickering emulsions

stabilized by chayote tuber starch-tea polyphenol composites," *Food Hydrocolloids*, vol. 172, 2026, Art. no. 112113, doi: 10.1016/j.foodhyd. 2025.112113.

[10] V. Ramos-Villacob, J. Salcedo-Mendoza, and J. A. Figueroa-Flórez, "Pickering emulsions stabilized by cassava starch–fatty acid complexes: A simple and dual ultrasound-assisted treatment strategy," *International Journal of Biological Macromolecules*, vol. 322, 2025, Art. no. 146908, doi: 10.1016/j.ijbiomac. 2025.146908.

[11] L. Chen, F. Ao, X. Ge, and W. Shen, "Food-grade Pickering emulsions: Preparation, stabilization and applications," *Molecules*, vol. 25, no. 14, 2020, Art. no. 3202, doi: 10.3390/ molecules25143202.

[12] W. Liu, J. Wang, D. J. McClements, and L. Zou, "Encapsulation of β-carotene-loaded oil droplets in caseinate/alginate microparticles: Enhancement of carotenoid stability and bioaccessibility," *Journal of Functional Foods*, vol. 40, Sep. 2018, pp. 527–535, doi: 10.1016/j. jff.2017.11.046.

[13] W. Ding et al., "Encapsulation of resveratrol by Pickering emulsion stabilized by *Pueraria lobata* nano-starch," *International Journal of Biological Macromolecules*, vol. 337, 2026, Art. no. 149557, doi: 10.1016/j.ijbiomac.2025. 149557.

[14] W. Xu, K. Lv, W. Mu, S. Zhou, and Y. Yang, "Encapsulation of α-tocopherol in whey protein isolate/chitosan particles using oil-in-water emulsion with optimal stability and bioaccessibility," *LWT*, vol. 148, Apr. 2021, Art. no. 111724, doi: 10.1016/j.lwt.2021.111724.

[15] Z. Mao et al., "Chitosan/octenyl succinic anhydride starch complex particles stabilize Pickering emulsion for astaxanthin encapsulation," *International Journal of Biological Macromolecules*, vol. 299, Aug. 2024, Art. no. 140056, doi: 10.1016/j.ijbiomac. 2025.140056.

[16] T. O. Hay, J. R. Nastasi, S. Prakash, and M. A. Fitzgerald, "Comparison of gidyea gum, gum arabic, and maltodextrin in the microencapsulation and colour stabilisation of anthocyanin-rich powders using freeze-drying and spray-drying techniques," *Food Hydrocolloids*, vol. 163, Jul. 2024, Art. no. 111023, doi: 10.1016/j.foodhyd.2024.111023.

[17] S. Zhan, M. He, Y. Wu, and J. Ouyang, "Improved light and ultraviolet stability of curcumin encapsulated in emulsion gels prepared with corn starch, OSA-starch and whey protein isolate," *Food Chemistry*, vol. 446, Feb. 2024, Art. no. 138803, doi: 10.1016/j.foodchem. 2024.138803.

[18] Z. Yang et al., "Fabrication and characterization of novel curcumin-loaded thermoreversible high amylose maize starch emulsion gel," *International Journal of Biological Macromolecules*, vol. 280, Jul. 2024, Art. no. 136173, doi: 10.1016/j.ijbiomac.2024.136173.

[19] E. Apostolidis, G. N. Stoforos, and I. Mandala, "Starch physical treatment, emulsion formation, stability, and their applications," *Carbohydrate Polymers*, vol. 305, 2023, Art. no. 120554, doi: 10.1016/j.carbpol.2023.120554.

[20] H. Mi, S. Liang, J. Chen, X. Li, and J. Li, "Effect of starch-based emulsion with different amylose content on the gel properties of *Nemipterus virgatus* surimi," *International Journal of Biological Macromolecules*, vol. 259, 2024, Art. no. 129183, doi: 10.1016/j.ijbiomac.2023.129183.

[21] A. A. Wani, P. Singh, M. A. Shah, U. Schweiggert-Weisz, K. Gul, and I. A. Wani, "Rice starch diversity: Effects on structural, morphological, thermal, and physicochemical properties—A review," *Comprehensive Reviews in Food Science and Food Safety*, vol. 11, no. 5, pp. 417–436, 2012, doi: 10.1111/j.1541-4337. 2012.00193.x.

[22] E. J. Vernon-Carter, C. Hernandez-Jaimes, M. Meraz, V. H. Lara, C. Lobato-Calleros, and J. Alvarez-Ramirez, "Physico-chemical characterization and in vitro digestibility of gelatinized corn starch dispersion fractions obtained by centrifugation," *Starch/Staerke*, vol. 67, no. 7–8, pp. 701–708, 2015, doi: 10.1002/star .201500074.

[23] X. Yan et al., "Influence factors of starch nanoparticles formation and their application in Pickering emulsion," *Food Bioscience*, vol. 54, Jul. 2023, Art. no. 102945, doi: 10.1016/j.fbio. 2023.102945.

[24] K. M. Albano and V. R. Nicoletti, "Ultrasound impact on whey protein concentrate-pectin complexes and in the O/W emulsions with low oil soybean content stabilization," *Ultrasonics*

Sonochemistry, vol. 41, 2018, pp. 562–571, doi: 10.1016/j.ultsonch.2017.10.018.

[25] Y. Shi, J. Cao, L. Li, and X. Yang, "Enhancing stability and performance of emulsion stabilized by soy protein isolate nanofiber - polysaccharide complexes," *LWT*, vol. 205, Apr. 2024, Art. no. 116495, doi: 10.1016/j.lwt.2024.116495.

[26] N. Wang, J. Cheng, Y. Jiang, Y. Meng, K. Zhang, Q. Ban, and X. Wang, "Emulsions stabilised by casein and hyaluronic acid: Effects of high intensity ultrasound on the stability and vitamin E digestive characteristics," *Ultrasonics Sonochemistry*, vol. 94, 2023, Art. no. 106340, doi: 10.1016/j.ultsonch.2023.106340.

[27] J. Xue and Y. Luo, "Protein-polysaccharide nanocomplexes as nanocarriers for delivery of curcumin: A comprehensive review on preparation methods and encapsulation mechanisms," *Journal of Future Foods*, vol. 3, no. 2, pp. 99–114, 2023, doi: 10.1016/j.jfutfo. 2022.12.002.

[28] Z. Lutfi, F. Alam, A. Nawab, A. Haq, and A. Hasnain, "Effect of NaCl on physicochemical properties of xanthan gum – water chestnut starch complexes," *International Journal of Biological Macromolecules*, vol. 131, pp. 557–563, 2019, doi: 10.1016/j.ijbiomac.2019.03.052.

[29] J. Bak, "A comparative study on the rheological properties of concentrated xanthan gum in combination with gum arabic or gum arabic-based emulsion," *International Journal of Biological Macromolecules*, vol. 265, Art. no. 131159, 2024, doi: 10.1016/j.ijbiomac.2024.131159.

[30] C. Zhang et al., "Effects of enhanced starch-xanthan gum synergism on their physicochemical properties, functionalities, structural characteristics, and digestibility," *International Journal of Biological Macromolecules*, vol. 241, Mar. 2023, Art. no. 124646, doi: 10.1016/j.ijbiomac.2023.124646.

[31] S. Liu et al., "Encapsulation in amylose inclusion complex enhances the stability and release of vitamin D," *Nutrients*, vol. 15, no. 5, 2023, Art. no. 1111, doi: 10.3390/nu15051111.

[32] Y. Zhang, B. Dou, J. Jia, Y. Liu, and N. Zhang, "A study on the structural and digestive properties of rice starch–hydrocolloid complexes treated with heat–moisture treatment," *Foods*, vol. 12, no. 23, 2023, Art. no. 4241, doi: 10.3390/ foods12234241.

[33] K. C. G. Silva and A. C. K. Sato, "Sonication technique to produce emulsions: The impact of ultrasonic power and gelatin concentration," *Ultrasonics Sonochemistry*, vol. 52, Dec. 2018, pp. 286–293, doi: 10.1016/j.ultsonch.2018.12.001.

[34] D. Gómez-Luría, E. J. Vernon-Carter, J. Alvarez-Ramirez, and F. Cruz-Sosa, "Insights of the ability of gelatinized fractions from non-chemical modified corn, rice, wheat, and waxy corn starches to stabilize O/W emulsions," *Food Hydrocolloids*, vol. 89, pp. 726–734, 2019, doi: 10.1016/j.foodhyd.2018.11.045.

[35] D. M. Ramos, V. Sadtler, P. Marchal, C. Lemaitre, L. Benyahia, and T. Roques-Carmes, "Properties of non-conventional direct O/W Pickering emulsions stabilized by partially hydrophobic silica particles controlled by rotor-stator or ultrasonic emulsification," *Colloids and Surfaces A: Physicochemical and Engineering Aspects*, vol. 673, Apr. 2023, Art. no. 131782, doi: 10.1016/j.colsurfa.2023.131782.

[36] J. O'Sullivan, B. Murray, C. Flynn, and I. Norton, "Comparison of batch and continuous ultrasonic emulsification processes," *Journal of Food Engineering*, vol. 167, pp. 114–121, 2015, doi: 10.1016/j.jfoodeng.2015.05.001.

[37] Q. Fu, H. Shi, L. Zhou, P. Li, and R. Wang, "Effects of ultrasound power on the properties of non-salt chicken myofibrillar protein emulsions," *International Journal of Food Science & Technology*, vol. 57, no. 4, pp. 2523–2534, 2022, doi: 10.1111/ijfs.15626.

[38] P. Salum, O. Güven, L. Y. Aydemir, and Z. Erbay, "Microscopy-assisted digital image analysis with Trainable Weka Segmentation (TWS) for emulsion droplet size determination," *Coatings*, vol. 12, no. 3, 2022, Art. no. 364, doi: 10.3390/coatings12030364.

[39] R. Yulianingsih and S. Gohtani, "Dispersion characteristics of pregelatinized waxy rice starch and its performance as an emulsifier for oil-in-water emulsions: Effect of gelatinization temperature and starch concentration," *Food Hydrocolloids*, vol. 95, pp. 476–486, 2019, doi: 10.1016/j.foodhyd.2018.12.013.

[40] Y. Shi, M. Zhang, K. Chen, and M. Wang, "Nano-emulsion prepared by high pressure

homogenization method as a good carrier for Sichuan pepper essential oil: Preparation, stability, and bioactivity," *LWT*, vol. 154, Nov. 2021, Art. no. 112779, doi: 10.1016/j.lwt.2021.112779.

[41] H. R. Sharif, M. K. Sharif, and F. Zhong, "Preparation, characterization and rheological properties of vitamin E enriched nanoemulsion," *Pakistan Journal of Food Sciences*, vol. 27, no. 1, pp. 7–14, 2017.

[42] N. Sharma, G. Kaur, and S. K. Khatkar, "Optimization of emulsification conditions for designing ultrasound assisted curcumin loaded nanoemulsion: Characterization, antioxidant assay and release kinetics," *LWT*, vol. 141, 2021, Art. no. 110962, doi: 10.1016/j.lwt.2021.110962.

[43] K. Kamwilaisak et al., "Rheology, stability, antioxidant properties, and curcumin release of oil-in-water Pickering emulsions stabilized by rice starch nanoparticles," *International Journal of Biological Macromolecules*, vol. 214, pp. 370–380, 2022, doi: 10.1016/j.ijbiomac.2022.06.032.

[44] L. Kong, U. Yucel, R. Yoksan, R. J. Elias, and G. R. Ziegler, "Characterization of amylose inclusion complexes using electron paramagnetic resonance spectroscopy," *Food Hydrocolloids*, vol. 82, pp. 82–88, 2018, doi: 10.1016/j.foodhyd.2018.03.050.

[45] P. Bernazzani, V. K. Peyyavula, S. Agarwal, and R. K. Tatikonda, "Evaluation of the phase composition of amylose by FTIR and isothermal immersion heats," *Polymer*, vol. 49, no. 19, pp. 4150–4158, 2008, doi: 10.1016/j.polymer.2008.07.022.

[46] H. Li, W. Zhang, L. Lin, X. Wu, and W. Wu, "Structural characteristics and emulsion stability of rice bran protein-chitosan complex: Effects of protein oxidation and ultrasonic treatment," *Food Chemistry*, vol. 490, 2025, Art. no. 145143, doi: 10.1016/j.foodchem.2025.145143.

[47] N. Aryanti et al., "Application of modified corn starch in stabilization of ultrasonic-assisted Pickering oil in water emulsion," *Food Research*, vol. 8, pp. 78–89, 2024, doi: 10.26656/fr.2017.8(S1).12.

[48] C. Kim, M. Seong, and A. Lee, "Fabrication of solid–liquid composites with highly uniform and size-controllable droplet inclusions," *Composites Communications*, vol. 64, 2026, Art. no. 102790, doi: 10.1016/j.coco.2026.102790.

[49] Y. Dai et al., "Formation and drying dynamics of cellulose nanocrystal capsules produced via double emulsion drops," *Colloids and Surfaces A: Physicochemical and Engineering Aspects*, vol. 733, 2026, Art. no. 139264, doi: 10.1016/j.colsurfa.2025.139264.

[50] K. D. Richards, E. Comish, and R. C. Evans, "Computer vision for high-throughput analysis of Pickering emulsions," *Soft Matter*, vol. 21, no. 12, pp. 2339–2348, 2025, doi: 10.1039/D4SM01252F.

[51] T. Zhang, M. Ding, X. Wang, and J. Zhong, "Droplet and creaming stability of fish oil-loaded gelatin/surfactant-stabilized emulsions depends on both the adsorption ways of emulsifiers and the adjusted pH," *Food Science and Human Wellness*, vol. 9, no. 3, pp. 280–288, 2020, doi: 10.1016/j.fshw.2020.04.002.

[52] N. Aryanti, A. R. Adina, A. Nafiunisa, and D. H. Wardhani, "Pea protein-based Pickering emulsions: Mechanistic insights into its modification and innovations for food applications," *Journal of Agriculture and Food Research*, vol. 19, Feb. 2025, Art. no. 101712, doi: 10.1016/j.jafr.2025.101712.

[53] S. A. Ledari, J. M. Milani, S. A. Shahidi, and A. Golkar, "Comparative analysis of freeze drying and spray drying methods for encapsulation of chlorophyll with maltodextrin and whey protein isolate," *Food Chemistry: X*, vol. 21, 2024, Art. no. 101156, doi: 10.1016/j.fochx.2024.101156.

[54] A. Magri, M. Ramos, C. Mellinas, A. Jiménez, and M. C. Garrigós, "Encapsulation of lemongrass essential oil in cyclodextrins and maltodextrin: Antioxidant, antimicrobial and release studies," *Carbohydrate Polymer Technologies and Applications*, vol. 10, Mar. 2025, Art. no. 100749, doi: 10.1016/j.carpta.2025.100749.

[55] M. Fathi, M. N. Nasrabadi, and J. Varshosaz, "Characteristics of vitamin E-loaded nanofibres from dextran," *International Journal of Food Properties*, vol. 20, no. 11, pp. 2665–2674, 2017, doi: 10.1080/10942912.2016.1247365.

[56] N. Yeasmen and V. Orsat, "Microencapsulation of ultrasound-assisted phenolic extracts of sugar maple leaves: Characterization, in vitro gastrointestinal digestion, and storage stability," *Food Research International*, vol. 182, 2024, Art. no. 114133, doi: 10.1016/j.foodres.2024.11 4133.

[57] D. Dahatonde et al., "Effect of heat treatment on physicochemical, interfacial, and encapsulation properties of pea and soy protein-based emulsions and their spray-dried powders," *Food Chemistry: X*, vol. 29, 2025, Art. no. 102791, doi: 10.1016/j.fochx.2025.102791.

[58] A. K. P. Jauhari, P. F. C. Wilms, M. N. Corstens, and M. A. I. Schutyser, "Encapsulating volatiles: The role of emulsion stability on the retention of d-limonene during emulsification and spray drying," *LWT*, vol. 223, 2025, Art. no. 117784, doi: 10.1016/j.lwt.2025.117784.

[59] H. Zhang et al., "Steroidal saponins and sapogenins from fenugreek and their inhibitory activity against α-glucosidase," *Steroids*, vol. 161, May 2020, Art. no. 108690, doi: 10.1016/j.steroids.2020.108690.